BIODIVERSITAS
Volume 24, Number 9, September 2023
Pages: 5044-5056

ISSN: 1412-033X
E-ISSN: 2085-4722
DOI: 10.13057/biodiv/d240948

Implementation of the Pelagic Hotspot Index in detecting the habitat suitability area for bigeye tuna (*Thunnus obesus*) in the eastern Indian Ocean

ZABHIKA DINDA ISTNAENI[1], JONSON LUMBAN GAOL[2,♥], MUKTI ZAINUDDIN[3], DEVI FITRIANAH[4]

[1]Graduate School of Marine Science and Technology, Institut Pertanian Bogor. Jl. Raya Dramaga, Bogor 16680, West Java, Indonesia
[2]Department of Marine Science and Technology, Faculty of Fisheries and Marine Science, Institut Pertanian Bogor. Jl. Raya Dramaga, Bogor 16680, Indonesia. Tel./fax.: +62-251-8622909, ♥email: jonson_lumbangaol@yahoo.com
[3]Faculty of Marine Science and Fisheries, Universitas Hasanuddin. Jl. Perintis Kemerdekaan Km. 10, Makassar 90245, South Sulawesi, Indonesia
[4]School of Computer Science, Universitas Bina Nusantara. Jl. Kebon Jeruk Raya No. 27, Jakarta 11530, DKI Jakarta, Indonesiata

Manuscript received: 11 June 2023. Revision accepted: 28 September 2023.

Abstract. *Istnaeni ZD, Gaol JL, Zainuddin M, Fitrianah D. 2023. Implementation of the Pelagic Hotspot Index in detecting the habitat suitability area for bigeye tuna (*Thunnus obesus*) in the eastern Indian Ocean. Biodiversitas 24: 5044-5056.* Bigeye tuna *(Thunnus obesus* Lowe, 1839*)* is a species with a high economic value that can migrate horizontally and vertically over a large area. Although sea temperature has been the main focus of previous findings, other variables can serve as a reasonable proxy. Here we used sea surface chlorophyll-a, sea surface height, subsurface sea salinity, and subsurface temperature to predict the suitable habitat area for bigeye tuna in the Eastern Indian Ocean Off Java. A Generalized Additive Model was performed to analyze the best-fit model evaluated from the *p*-value and Cumulative Deviance Explained. The suitability index of the selected model was calculated using Pelagic Hotspot Index constructed from multi-spectrum satellite data. The results showed that the high catches were located on the high suitable index value and supported by chlorophyll-a as the most significant factor, followed by sea surface height, temperature, and salinity. This condition was stimulated by the high feeding opportunity, which may relate to the EIO's oceanic front, eddies, and specific current patterns. This study helps identify ecological hotspots, track the migration, and monitor the seasonal closure for bigeye tuna, particularly in EIO.

Keywords: Bigeye tuna, GAM, GIS, habitat suitability, Pelagic Hotspot Index

Abbreviations: EIO: The Eastern Indian Ocean; SSC: Sea Surface Chlorophyll-a; SSH: Sea Surface Height; sub-SS: Subsurface Salinity; sub-ST: Subsurface Temperature; HR: Hook Rate, GAM: Generalized Additive Model; PHI: Pelagic Hotspot Index; CDE: Cumulative Deviance Explained; AIC: Akaike Information Criterion

INTRODUCTION

In the Indian Ocean, bigeye tuna (*Thunnus obesus* Lowe, 1839) is the third most valuable catch (~9%) after skipjack (~53%) and yellowfin tuna (~38%) (IOTC 2021). This species is distributed from the surface layer with temperatures exceeding 20°C on daily vertical movement, descending to depths of 500 m where the water column temperature is considerably cooler (~5°C) and encountered within the mixed layer during the nighttime (Holland and Sibert 1994; Block and Stevens 2001; Brill et al. 2005). It is dominantly caught by longline tuna vessels operating in the Indian Ocean between 30°S and 20°N (Arrate et al. 2021).

Despite having a broad swimming ability both horizontally and vertically, an adequate evaluation of the dynamics of tuna movement in the subsurface waters of the eastern Indian Ocean (EIO) has not been conducted, while this has been studied through tuna tagging technology in the Pacific (Senina et al. 2019; Schaefer and Fuller 2022) and Atlantic (Wright et al. 2021; Gaertner et al. 2022) oceans. This requires more accurate and comprehensive fishery data statistics to improve monitoring and stock evaluation of existing species, specifically their swimming depth.

One way to understand the dynamics of the bigeye tuna movement is to identify the characteristics of its preferred water conditions. The EIO waters are very complex because it is influenced by several wave systems (Syamsuddin et al. 2013) and climate variability (Kumar et al. 2014; Wang and Wang 2014; (Kim and Na 2022). Scientists have done numerous studies to figure out how tuna interacts with its surroundings. Salinity affects density and water circulation, indicates climate in a water area (Vinogradova et al. 2019), and affects tunas distribution. The temperature at a certain depth affects tuna catches (Cai et al. 2020). Sea surface height anomalies show a dominant signal of bigeye tuna seasonal and annual variability (Gaol et al. 2015). Not only oceanography variables, climatic phenomena like El Nino Southern Oscillation (ENSO) and Indian Ocean Dipole (IOD) affect pelagic fish catches (Baharuddin et al. 2022).

Generalized Additive Models (GAM) are well suited for creating ecological models with highly complex data because they can handle non-linear connections between variables (Guisan et al. 2002). It is a method with high

performance and better accuracy in examining tuna habitat utilization (Mugo and Saitoh 2020; Zainuddin et al. 2023) and enhancing the understanding of the ecological system through fisheries data and environmental variables (Setiawati et al. 2015).

Another challenge in tuna fisheries is the pressure due to the increasing demand in the market that threatens resource sustainability. Therefore, to achieve better management, determining potential tuna habitats helps to reach sustainable fisheries. Several studies have used empirical habitat modeling with Habitat Suitability Index (HSI) (Haghi et al. 2016; Lee et al. 2018; Lee et al. 2020) or maximum entropy (Syah et al. 2016; Zhang et al. 2021) to predict the potential fish habitats. The Pelagic Hotspot Index (PHI), first implemented by Zainuddin et al. (2017), is one approach that has not been widely implemented. Compared to others, this method considers the relationship between oceanographic parameters with fish abundance index and fishing effort frequency in detecting the spatial pattern.

Based on what has been explained above, it is known that (i) research on tuna in EIO still rarely considers subsurface data in determining potential fishing areas, (ii) the implementation of the PHI method has never been carried out in similar studies in EIO, and (iii) there are chances for the oceanographic factors and climatic phenomena in forming the preferable area of bigeye tuna. Therefore, this study aims to evaluate the relationship between bigeye tuna and various oceanographic parameters by combining surface and subsurface data and to predict its potential habitats based on oceanographic conditions in the EIO.

MATERIALS AND METHODS

Study area

The study area covered the region of Eastern Indian Ocean (EIO) - Off Java (105°-122.59°E and 5.28°-20°S, Figure 1). The EIO is considered a complex region (Behera et al. 2013) where many dynamic currents and wave systems influence this area (Syamsuddin et al. 2013), such as South Java Current (SJC), South Equatorial Current (SEC), and Indonesian Throughflow (ITF). The ITF plays a vital role in climate heat transfer (Meyers 1996) and also the climate phenomenon such as Indian Ocean Dipole (IOD) and El Nino Southern Oscillation (ENSO).

Procedures

Data collection

Bigeye tuna catches were collected from the logbooks of longline tuna fleets operated in the Southeast Indian Ocean under PT. Perikanan Nusantara, the Incorporated Fishing Company of the Indonesia Government based in Benoa, Bali, Indonesia. The fishing data consist of longitude, latitude, and bigeye tuna catch (tails), recorded daily from January 2009 to December 2010. These data were digitized and compiled into monthly data to match the temporal resolution of the satellite imagery and model employed.

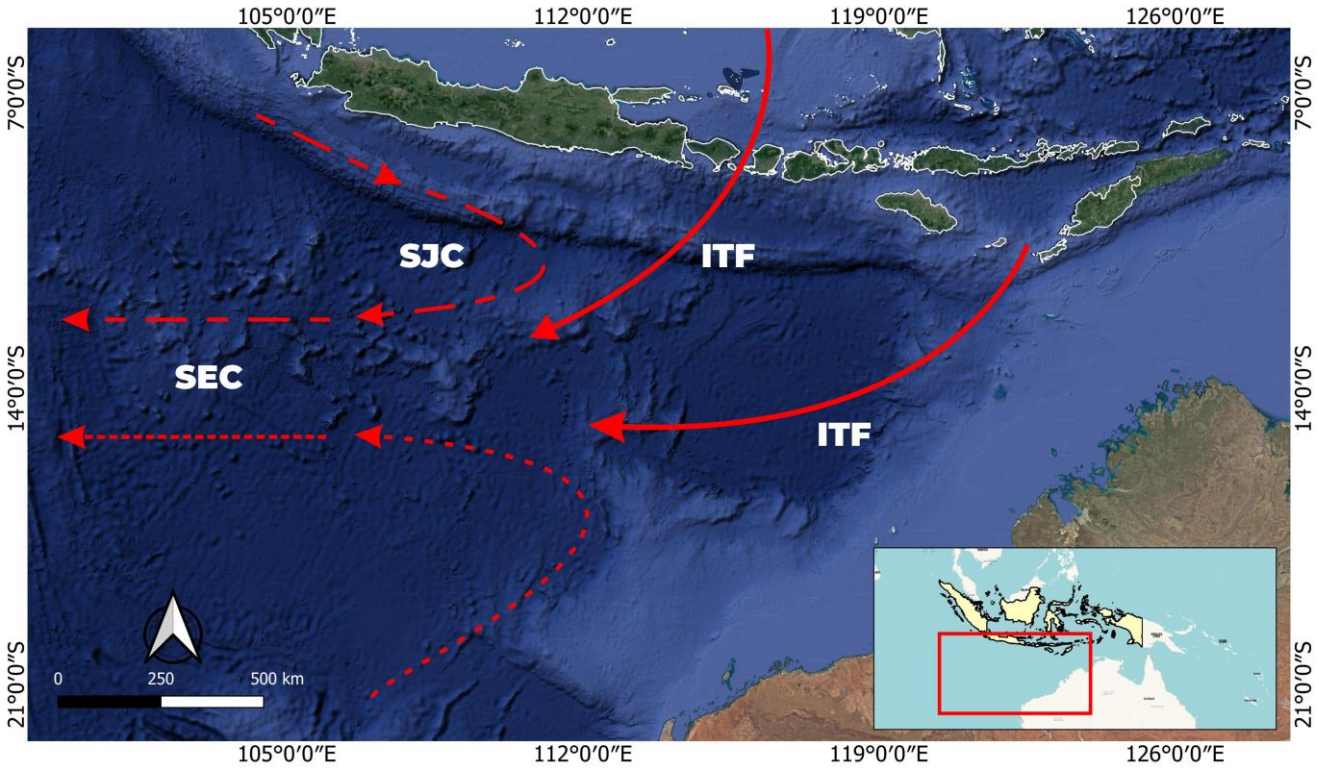

Figure 1. Study area map in the Eastern Indian Ocean (EIO) off the Java (modified from Syamsuddin et al. 2013 and Gingele et al. 2002)

The hook rates of bigeye tuna (HR) were computed by dividing the number of fish caught per 100 hooks operated based on each georeferenced fishing position. HR were used as an indicator in assessing the abundance and exploitation rate of fish (Bahtiar et al. 2013) and have been applied to previous longline studies in the same area (Nugraha and Triharyuni 2009; Nugraha and Hufiadi 2012; Jatmiko et al. 2014). The data were divided into train and validation datasets. We used the dataset of 136 longline fishing points in October, November, and December 2010 to validate the model.

Oceanographic parameter data comprised sub-surface temperature, sub-surface salinity, surface chlorophyll-a, and sea surface height. The data at a depth of 200 m were selected for several reasons. Apart from being within the range of the fishing gear employed, it is also based on previous research indicating that bigeye tuna habitats are at depths exceeding 150 m (Nugraha and Hufiadi 2012) and at a depth of 222 m were predicted to have a broader area with a high value of HSI (Syah et al. 2019). We used sub-surface data at 200 m for both temperature and salinity from the GLORYS12V1 model (https://data.marine.copernicus.eu/product/GLOBAL_MULTIYEAR_PHY_001_030/services) to enhance our understanding of bigeye tuna at a specified swimming layer. The surface chlorophyll-a data were obtained from Moderate Resolution Imaging Spectro-Radiometer (MODIS) Aqua SMI L3 (https://oceancolor.gsfc.nasa.gov/l3/). We also use weekly current data from LAS AVISO (https://las.aviso.altimetry.fr/las/) compiled into monthly resolutions to support the research findings. The data specifications are shown in Table 1.

According to the quality information document the GLORYS12V1 product, the temperature remains consistent with Root Mean Square Error (RMSE) values less than 0.4°C throughout the water column in the equatorial region. The increasing thermal structure, in correlation with the deployment of Argo floats, particularly in layers below 300 meters, exhibits a bias approaching 0°C and an RMSE value from in-situ measurements generally less than 1°C. Salinity data demonstrates an average bias close to zero globally, with a common bias of less than 0.1 psu in the 50-200 m layer (CMEMS, accessed).

Data analysis

Satellite and fishing data processing

SSC from MODIS Aqua was processed with SeaDAS 8.0.0 (NASA Goddard Space Flight Center, Greenbelt, MD) to extract the geography information. The sub-ST, sub-SS, SSH, and SSC images were then reprojected to align the spatial resolution. The distribution of interpolated data was mapped using ArcGIS 10.8 (ESRI, Redlands, CA) to see the trends for each parameter. The Kriging method did the image interpolation, which was more reliable than the conventional interpolation techniques used in GIS (Oliver and Webster 1990). The fishing data were plotted and overlayed on the interpolated image with the match temporal resolution. Extraction was carried out to obtain the value of the oceanographic variables for each fishing point.

The best-fit model using Generalized Additive Model (GAM)

The best-fitted model was used to evaluate habitat suitability. We built several combinations of parameters used to find the best model fit. The preferred model of oceanographic parameters for bigeye tuna was obtained using Generalized Additive Model (GAM). GAM has been defined as an extension of the class of generalized linear models that utilize the adaptability of nonparametric regression (Hastie and Tibshirani 1990). In many modeling scenarios, GAM analytical technique offers numerous ways to discover covariate effects (Hastie and Tibshirani 1987). Researchers have used this method to analyze the relationship between oceanographic parameters and fish species (Zainuddin et al. 2008; Syamsuddin et al. 2013; Setiawati et al. 2015; Safruddin et al. 2022). GAM wrote:

$$g(\mu_i) = f_1(x_{1_i}) + f_2(x_{2_i}) + f_3(x_{3_i}) + \cdots \quad (1)$$

Where:

g : The link function
μ_i : The expected result of the dependent variable
f_i : Smoothing function
x_i : Independent variable

In this method, we utilized the gam function in the *mgcv* package (Wood 2017) in R Studio 2022.02.0+443 (posit, Boston, MA) to build GAMs. The HR of the bigeye tuna served as the dependent variable, while the SSC, sub-ST, sub-SS, and SSH were designated as the independent variables. Each model was evaluated using Cumulative Deviance Explained (CDE), the significance of *p*-value, and Akaike Information Criterion (AIC). AIC provides a way to select the best set of models where the best set has the minimum score (Johnson and Omland 2004). The model with the highest CDE percentage, the most significant *p*-value, and the lowest AIC value was chosen as the most appropriate.

Table 1. Specification of the oceanography parameters

Oceanographic data	Abbreviation	Product	Temporal resolution	Spatial resolution	Source
Sea temperature at 200 m (°C)	sub-ST	GLORYS12V1	Monthly	0.083°×0.083°	Copernicus
Sea salinity at 200 m (psu)	sub-SS	GLORYS12V1	Monthly	0.083°×0.083°	Copernicus
Sea surface height (m)	SSH	GLORYS12V1	Monthly	0.083°×0.083°	Copernicus
Sea surface chlorophyll-a (mg m^{-3})	SSC	Aqua-MODIS L3	Monthly	4 km	Ocean Color
Currents (m/s)		AVISO-Delayed time global altimetry	Weekly	25 km	LAS AVISO

Habitat suitability model using Pelagic Hotspot Index (PHI)

The habitat suitability maps were created by calculating the suitability index value from the chosen model with the PHI, where the HR, the frequency of fishing efforts, and their relation to oceanographic parameters were considered. The total HR and fishing frequencies at a particular interval of the histogram were divided by the maximum total HR from the class interval of the oceanography parameters (sub-ST, sub-SS, SSC, and SSH) (Eq 1 and 2). The maximum value of HR or fishing frequency was then used as the standard, and the interval ranges of the variables were used to calculate the average suitability index (Eq 3). PHI wrote as (Zainuddin et al. 2017):

$$PI_{HR} = \frac{\sum \frac{HR_{ij}}{HR_i max}}{n} \quad (2)$$

$$PI_F = \frac{\sum \frac{F_{ij}}{F_i max}}{n} \quad (3)$$

$$PHI = \frac{(PI_{HR} + PI_F)}{2} \quad (4)$$

Where:

PI_{HR} : The probability value based on HR relation with oceanographic parameters

PI_F : The probability value based on the frequency of the HR

HR_{ij} : HR values on oceanographic parameters-*i* for class interval-*j*

$HR_i\ max$: The maximum value of HR on the oceanographic parameter-*i*

F_{ij} : The fishing frequency in oceanographic parameter-*i* for class interval-*j*

$F_i\ max$: The maximum value of fishing frequency on the oceanographic parameter-*i*

n : the total number of variables

The suitable index ranged from 0 to 1, where 1 is rated as the most suitable. Refers to Zainuddin et al. (2017), PHI with 0.75 (Quartile 3) or higher was considered as suitable as the bigeye tuna potential habitat.

Thermal and chlorophyll-a front

To support the results, thermal and chlorophyll-a fronts detection was carried out. The front area was detected using the SIED (Single Image Edge Detection) algorithm using the MGET (Marine Geospatial Ecology Tools) plugin in ArcGIS. This analysis used sub-ST and SSC satellite images.

Current speed and directions

The current speed and directions were measured to detect the eddy events. The meridian and zonal components were calculated using the equation:

$$c = (u^2 + v^2)^{1/2} \quad (5)$$

Where:

u : meridian value

v : zonal value

Model validation

This validation aims to measure how well the Pelagic Hotspot Index (PHI) method identifies potential areas for tuna presence by using the validation dataset outside the training dataset used in the built model. The fishing points were layered on a map of the suitability of the bigeye tuna habitat that had been formed with a class range of 0 to 1 and then extracted. The results of this extraction were used to evaluate the performance by observing whether the validation points were in the areas with a high predicted habitat suitability value. The fishing point with its HR value indicates the presence of bigeye tuna in the field. The extracted values from the validation points are then mapped in the distribution graph. The distribution diagram of the extracted PHI values was depicted using Origin 2018 64Bit (OriginLab, Northampton, MA). It was used to identify the PHI value where bigeye tuna was caught.

RESULTS AND DISCUSSION

Bigeye tuna and its oceanographic parameters distribution

The monthly average of bigeye tuna HR from longline vessels in 2009 and 2010 is shown in Figure 2. Based on the distribution chart, it is known that the peak catch season is in July and August with the average of 0.39 and 0.44, which in the EIO - Of Java is included in the east monsoon period. The lowest HR was in March and April for an average number of 0.20 and 0.21, respectively.

Figure 2 indicates the temporal fluctuation of HR data in the period of 2009-2010. Rochman et al. (2018) documented that between 2009 and 2010, industrial-scale tuna fishing activities experienced a decline of 41%. The number of vessel units landing at Benoa Port decreased from 1,850 units in 2009 to 1,099 units in 2010. This reduction in fleet size was a consequence of fleet reduction and operational days impact due to the rise in oil prices. The catching activities by the tuna longline fleet occurred offshore, far from the coastline, necessitating a substantial amount of fuel. Hapsari (2006) mentioned that as a result of this oil price increase, the total production of tuna longline fisheries owned by PT. Perikanan Nusantara decreased by 14.37% compared to the preceding year.

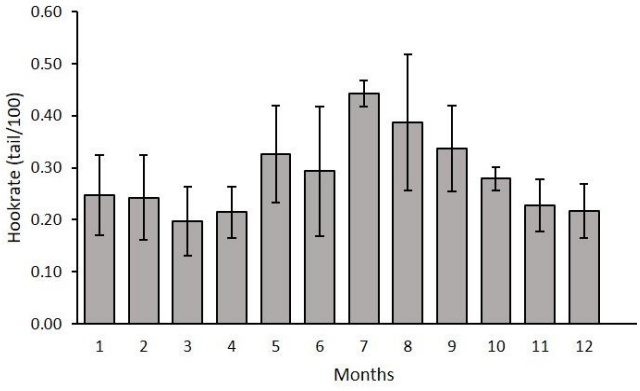

Figure 2. Monthly average of *T. obesus* HR from tuna longlines in EIO Off Java in 2009 and 2010

Figure 3 shows the average monthly distribution of oceanographic parameters in 2009 and 2010. Based on the distribution chart, it is known that oceanographic parameters constantly fluctuate. Entering the east season period, there was a decrease in sub-SS concentration and the lowest in July. The sub-SS levels rise quickly in August to September. The sub-ST at a depth of 200 m experiences an increasing trend during the peak catch season and has the highest number in August. The SSC concentration was low in the early months and slowly rose until it reached the highest concentration in August. The same case occurs for SSH, where the low height trend was in the first 4 months and rose until it peaked in June.

In the observed pattern of average distribution, it is evident that sub-ST and SSC exhibit a positive correlation with each other. Generally, when the concentration of SSC increases, the sub-ST tends to decrease due to the occurrence of upwelling processes that bring nutrient-rich cold water to the surface. In other words, it exhibits a negative correlation. This phenomenon is attributed to the existence of a more intricate relationship between the SSC concentration and the sub-ST. Upwelling events and other factors such as currents, atmospheric influences, and thermocline structure influence this relationship.

Oceanographic preferences for bigeye tuna

Figure 4 shows the bigeye tuna catch data distribution for each oceanographic parameter. Bigeye tuna were identified to be distributed at sub-SS between 34.4 to 35.1 psu, with a data frequency increased from 34.5 psu and decreased after the peak at 34.65-34.7 psu (Figure 4.A). The data distribution for sub-ST varied, ranging from 12 to 17.5°C, with the peak catch rate occurring at 16-16.5°C. There was a slight disparity in the data between sub-ST of 14.5 to 16°C where the fishing efforts frequency occurred below 600 (Figure 4.B). The distribution of SSC has the most comprehensive range among the other three parameters. It ranged from 0.05 to 0.25 mg m^{-3}, with the highest intensity at 0.07 mg m^{-3} and gradually decreasing after that (Figure 4.C). The gap between bars was little because SSC concentrations in offshore waters tended to be lower than in coastal waters. Lastly, the catch points were distributed between 0.45 to 0.9 m at SSH. It gradually increases until 0.7 m and decreases, with the highest frequency at SSH of 0.65 m (Figure 4.D).

Based on the GAM analysis, from the seven models built, we obtained that the best model fit is model 7 (Table 2), which combined the sub-ST, SSC, sub-SS, and SSH with a CDE value is 9.36% and the lowest AIC value (-213.4801). Table 2 showed that most model variables were highly significant (P <2e-16). This model with the highest CDE value was then used to calculate the suitability index value by analyzing each oceanographic parameter's weight. The table also shows that for the chosen model, SSC is the most influential among the four variables, followed by sub-ST, SSH, and sub-SS.

The percentage of unexplained variance indicates the presence of additional explanatory factors that may influence the distribution of bigeye tuna beyond the oceanographic parameters utilized in this study. Several variables such as eddy kinetic energy (EKE) and dissolved oxygen concentration (Zhang et al. 2021), climate variability like ENSO and IOD (Gaol et al. 2002), and the influence of current systems also has been considered in explaining the distribution of tuna.

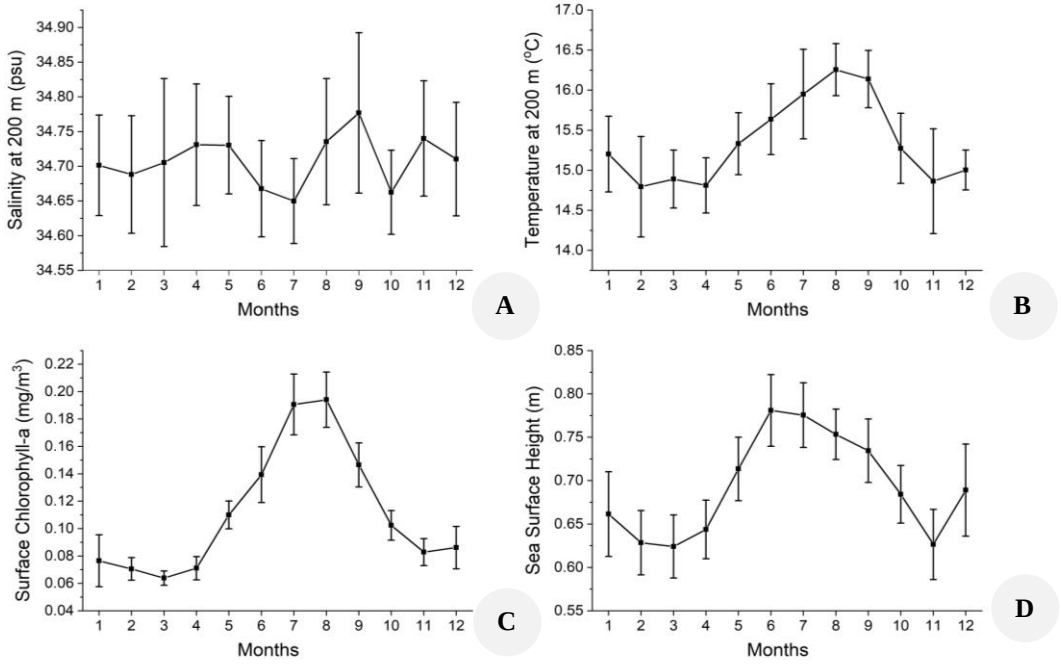

Figure 3. Average trend distribution for : A. sub-SS; B. sub-ST; C. SSC and; D. SSH in 2009 and 2010

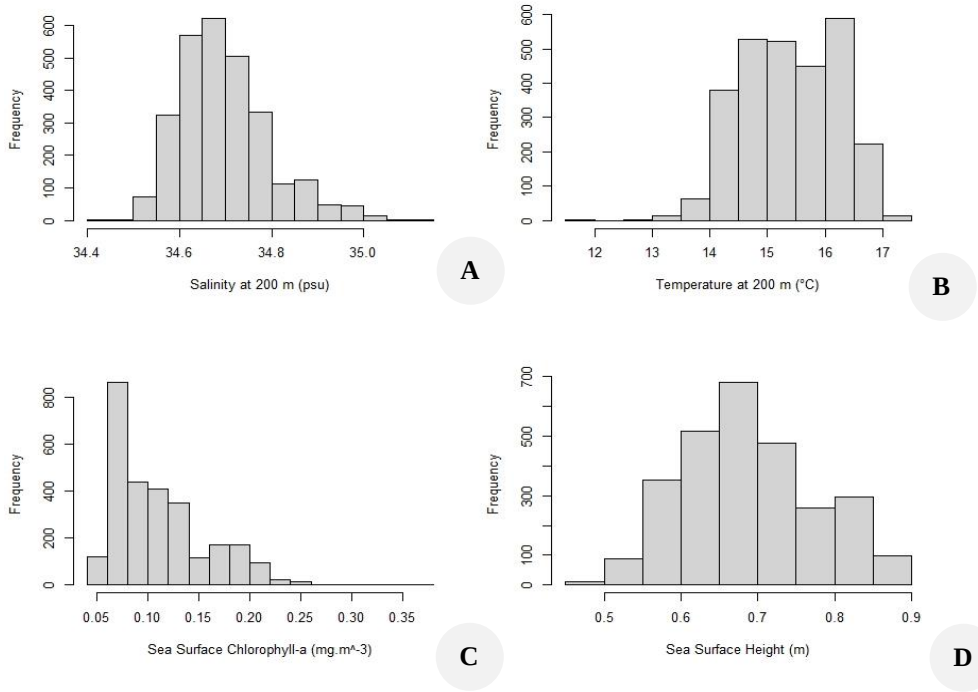

Figure 4. Graphic distribution of *T. obesus* HR frequency based on the oceanography parameters for: A. sub-SS; B. sub-ST; C. SSC, and; D. SSH in 2009 and 2010

Table 2. GAMs statistics result from HR of *T. obesus* in the EIO-Off Java on its relationship to oceanographic parameters

Model	p-value	CDE	AIC
sub-ST	<2e-16 ***	5.17%	-123.5506
SSC	<2e-16 ***	6.35%	-153.7296
sub-SS	0.000909 ***	0.735%	-2.601043
SSH	<2e-16 ***	4.58%	-115.6808
sub-ST	<2e-16 ***	7.88%	-188.4608
SSC	<2e-16 ***		
sub-ST	1.39e-05 ***	8.31%	-190.8653
SSC	< 2e-16 ***		
sub-SS	0.158		
sub-ST	0.0581.	9.36%	-213.4801
SSC	<2e-16 ***		
sub-SS	0.0203 *		
SSH	0.0001 ***		

Note: Sig. codes: 0 '***' 0.001 '**' 0.01 '*' 0.05 '.'

The GAM plots were created to interpret the specific impact of each predictor variable on the HR of bigeye tuna. The graphic response of bigeye tuna catches to each environmental parameter is shown in Figure 5. The dashed lines represent the uncertainty or variability of the model estimates, which constitute confidence intervals used to depict the extent to which the model can fluctuate, bounded by the upper and lower limits provided. A wider confidence interval indicates higher uncertainty, while a narrower interval signifies higher certainty. The GAM plot for sub-SS showed less fluctuation where the trend ranged from 34.5-35 psu (Figure 5.A). A significant effect on the catch rate of bigeye tuna occurred at sub-ST ranging from 13.5-17°C with a positive response from 15-16°C (Figure 5.B), while a negative effect occurred at the number lower than 13.5°C. Regarding SSC, the response concentrations ranged from 0.05 to 0.40 mg m^{-3}, followed by a negative trend with the HR appearing to increase on SSC 0.13-0.19 mg m^{-3} (Figure 5.C). The plot for SSH fluctuated slightly, where the trend occurred between 0.5-0.9 m (Figure 5.D).

SSC shows the data spread over quite a wide range of numbers, from 0.05-0.22 mg m^{-3}, where the range 0.06-0.07 mg m^{-3} dominated. The catch frequency ranged from 0.5 to 0.9 m and was highest at SSH between 0.65-0.7 m. Based on the distributed data, it can be interpreted that the preferred oceanographic condition for bigeye tuna is in the area with sub-SS ranging from 34.6-34.7 psu, sub-ST at 16-16.5°C, SSC at 0.06-0.07 mg m^{-3}, and SSH ranged from 0.65 to 0.7 m.

Suitable habitat for bigeye tuna in the eastern Indian Ocean

Following the weighting of each sub-ST, sub-SS, SSC, and SSH, Figure 6 shows the demonstration of the distribution of potential bigeye tuna habitats throughout the peak season, which occurs in June, July, and August, where the red area was considered as the highly chance of bigeye tuna to be likely to be present. According to their distribution, places with a high PHI are primarily found between 12° to 15°S and 108° to 122°E, where the waters around South Java have a lower PHI value than the nearby waters. However, the projection of bigeye tuna potential area began to narrow to 12° to 13°S region in August 2010. The PHI decreased in August 2010 because of the decay of eddy events. This implied to the decreasing of fishing points in high PHI area during the period. Apart from that, it is strongly suspected that catch points gather in this area due to front activity that is developing and stimulating feeding opportunity for bigeye tuna.

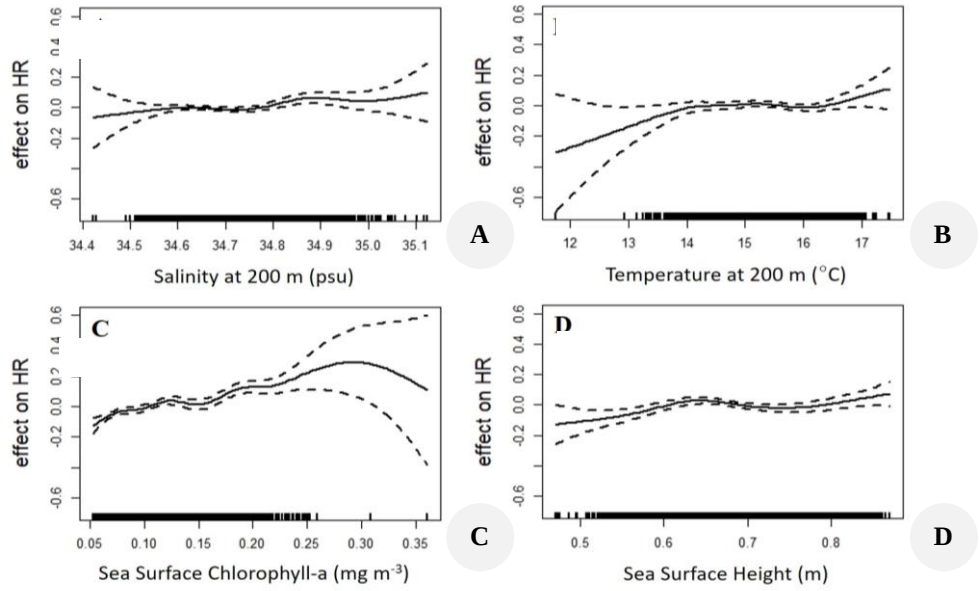

Figure 5. The response graph between the HR of *T. obesus* with oceanographic variables derived from the generalized additive models (GAMs) analysis. The solid line indicates the fitted function, and the thick line below shows the data distribution for (A) sub-SS, (B) sub-ST, (C) SSC, and (D) SSH in 2009 and 2010

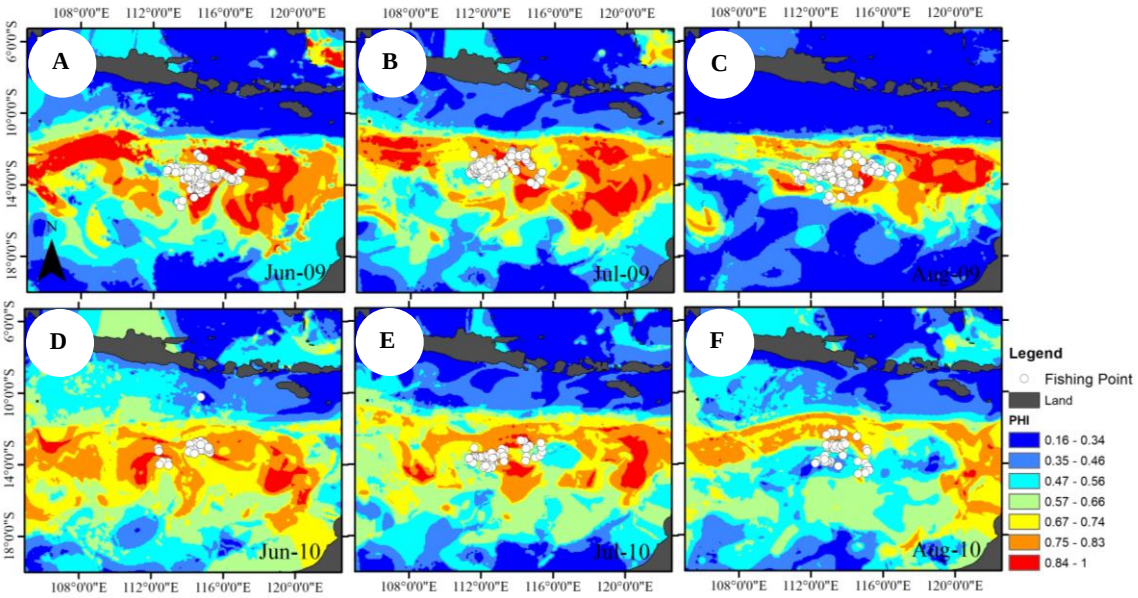

Figure 6. The spatial distribution for predicted *T. obesus* habitat hotspots maps obtained from Pelagic Habitat Index (PHI) for peak season in (A, B, C) June, July, and August 2009 and (D, E, F) June, July, and August 2010. White circles are the fishing points of longline vessels each month

Figure 7 shows the habitat suitability map prediction for bigeye tuna in October, November, and December 2010, overlain with the SSC, sub-ST, sub-SS, and SSH distribution for the exact temporal resolution, respectively. The distribution of sub-SS has increased in concentration towards the subtropical regions throughout October, November, and December (Figure 7.D, 7.E, and 7.F). The distribution of sub-ST showed a similar distribution pattern to sub-SS, where the closer to the low latitudes, the hotter the sub-ST. However, along the region of 12°S, there is a reasonably significant change from low to high sub-ST horizontally, as occurs at sea level (Figure 7.G, 7.H, 7.I).

The SSC image shows the concentration was increased on the south coast of Java (Figure 7.J, 7.K, and 7.L). SSH shows a significant difference where the area near and around the coast of Java shows a lower sea level than the area below it (12°-15°S), which has a higher sea level than the surrounding areas (Figure 7.M, 7.N, and 7.O). The region where the increase in SSC occurs is an area with a low SSH, as seen when comparing it to the SSH image.

The same case also occurred in a study conducted by Gaol et al. (2015), who found the distribution pattern of SSC concentrations following the SSH pattern. Based on the prediction map of habitat suitable area of bigeye tuna (Figure 7.A, 7.B, and 7.C), it is known that the validation points are generally in areas with high index values. In October, the areas predicted as most suitable for bigeye tuna are at 11°-15°S and 108°-122°E, in November at 11°-15°S and 108°-120°E., and in December is at 11°-15°S and 110°-122°E. The results also indicate there were potential habitat area of bigeye tuna outside the validation point that have chances to be explored.

The distribution of PHI examination towards the fishing point in October-December 2010 is shown in Figure 8. From the total validation point, more than half of the data has a value greater than 0.7. A total of 22 data has the range of PHI 0.75-0.8, 31 points in the range 0.80 - 0.85, 14 points in the range 0.85-0.9, and 24 points in the range 0.9-0.95. The result indicates a good consideration for other studies to implement this method in determining the bigeye tuna habitat preferences.

An indication of the excellent performance of this method in determining habitat suitability for bigeye is assessed from the high PHI value, area of suitable habitat, and persistence of the most suitable habitat (Zainuddin et al. 2017). The formation of a suitable area at this location is probably related to other phenomena supporting the formation of water conditions favored by bigeye tuna.

Relationship between fronts and eddies event with the formation of suitable habitat for bigeye tuna

The sub-ST distribution formed a horizontal gradient pattern that generally became a sign that there may be fronts in the area. Fronts typically create horizontal gradations in the water, which may be seen from oceanographic variables like temperature from satellite measurements (Chapman et al. 2020). The results from thermal front detection using SIED (Figure 9) from the six peak months (June, July, and August for 2009 and 2010) show the front occurred at 11°-13°S and is about 224 - 500 km from the mainland. The map shows that these fronts were detected near bigeye tuna catch areas.

In a recent study by Hidayat et al. (2019), the closer a fishing point to the front area, the higher the probability of catching more fish. Zainuddin et al. (2021) also found that a potential catch area for skipjack tuna in the Flores Sea has formed around a thermal front area 0-40 km from that location. We align with these as the results coincide with Cai et al. (2020), which observed that the high tuna catch area was in a sub-ST front ranging from 150-200 m. We also indicate that the fronts occurring within the study area are significantly influenced by the current systems operating in the water column. A study conducted by Sudre et al. (2023) states that the front peaks between 100 and 200 meters below the mixed layer suggest that they are primarily related to features of ocean dynamics rather than to mixed layer processes.

Figure 10 shows the SSC fronts in August 2009, where the fronts formed along the eastern waters off the coast of Java, Lombok Strait, and Nusa Tenggara Waters. The fishing locations were between the two constructed fronts, with some in the front region and the others in nearby places. The SSC fronts appeared as a form of response to upwelling events in the same area along with the detected eddies (Figure 11). The role of the wave system in this area is one of the factors for the distribution of bigeye tuna in this area. The confluence of currents with different characteristics triggers the occurrence of eddies and fronts. Fronts were often called hotspots for marine life since they typically are regions with greater levels of biodiversity and enhanced primary and secondary productivity (Belkin 2021; Scales et al. 2014). The link between the front and the bigeye tuna has also been explained in a study by Lan et al. (2021), where the formation of the front area affects the existence of prey organisms for immature bigeye tuna such as Pacific saury and neon flying squid.

A part of the EIO within the study area falls under Indonesia's Exclusive Economic Zone (EEZ), located within the Fisheries Management Area (FMA) 573. According to Nurani et al. (2018), there are numerous problems faced by FMA 573, such as the symptoms of overfishing due to the declining trend of Catch Per Unit Effort (CPUE), the use of illegal Fishing Aggregating Devices (FADs), unreported information of improper fishing technology, etc. The Indonesian government has established the Ocean Accounts of Indonesia program, which organizes social, economic, and environmental information to achieve the sustainable development of the ocean. One of the main projects within this initiative is the Quota-Based Fisheries program, which will be implemented in each FMA, including FMA 573. Steps in the implementation of this project involve the utilization of secondary data from institutions and global datasets, including satellite imagery, and preparing accounts on fish resources as individual ecosystem assets in creating the extent of area, condition, and monetary values of marine resources (MMAF 2022).

Additionally, it is thought that the presence of eddies in the area has a part in influencing the establishment of the bigeye potential habitat area. Figure 11 shows an overview of the formation of eddies around the fishing point in peak seasons (June, July, and August) in 2009 and 2010. Similar to fronts, eddies typically have embedded frontal interfaces and systems for converting the physical energy of the ocean system into trophic energy to support biological activity (Bakun 2006). This vortex can act as a tool to indicate the occurrence of upwelling, where a layer of cold water rises and carries nutrients up to the surface. The availability of abundant nutrients can be a favorite area of fish that have the potential to become prey for bigeye tuna. This condition was supported by previous studies that found that the Southeast monsoon period from June to August associated with El-Niño and positive IOD events in the southern waters of Indonesia triggered the upwelling causing the nutrients, including the concentration of chlorophyll-a, to increase. The ENSO and IOD phenomena that occur in the EIO influence the existence of tuna through the dynamics of changes in the distribution of oceanographic parameters (Sambah et al. 2023).

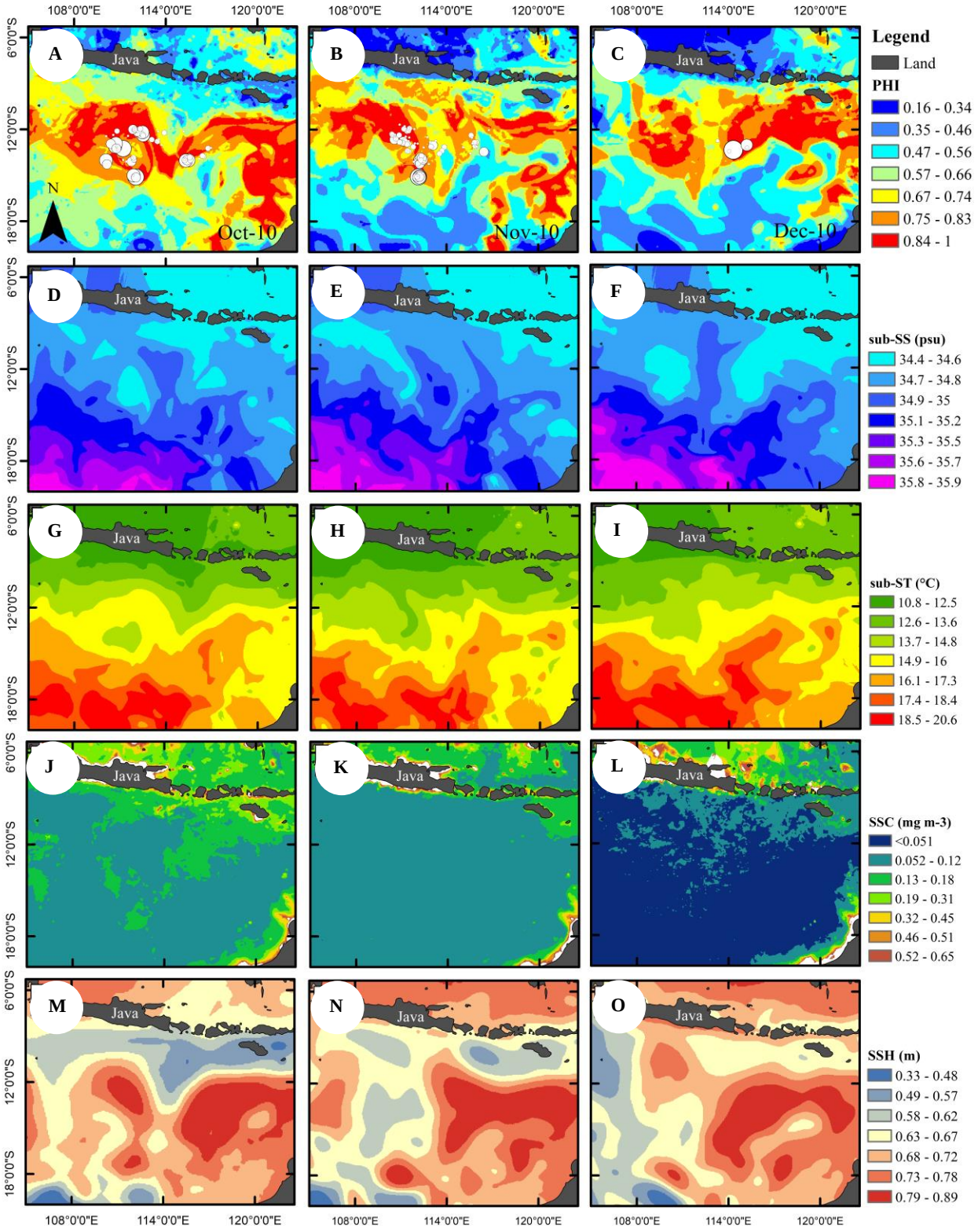

Figure 7. The spatial distribution for predicted *T. obesus* habitat hotspots maps obtained from PHI in A. October 2010; B. November 2010, C. December 2010 weighted from 0 to 1, followed by the oceanographic conditions for (D, E, F) sub-SS at 200-meter depth, (G, H, I) sub-ST at 200-meter depth, (J, K, L) SSC, and (M, N, O) SSH during October, November, and December 2010, sequentially. White circles are the fishing points of longline vessels each month

The current trend figure describes the confluence of several currents flowing into this region such as ITF. Gordon (2005) characterizes the ITF as a "mix-master," where the characteristics of water masses originating from the southern Pacific Ocean intermingle with the existing water masses within Indonesian waters, influencing temperature and salinity. The flow of ITF, passing through the Makassar Strait and entering the Indian Ocean through the Lombok Strait, extends to depths of up to 300 meters. This also explained one of the factors why the distribution trend of sub-SS and sub-ST (Figure 3) fluctuated.

Bigeye tuna schools are frequently spotted around plankton and micro-nekton concentrations, enabling this species to live in regions with significant upwelling productivity (Setiawati and Miura 2014). The presence of nutrients, the temperature of the water, and ocean currents are only a few of the variables that affect chlorophyll-a concentration in the sea. It is critical to remember that, like many ecological interactions in marine ecosystems, the one between chlorophyll-a and bigeye tuna can be complex and influenced by various factors.

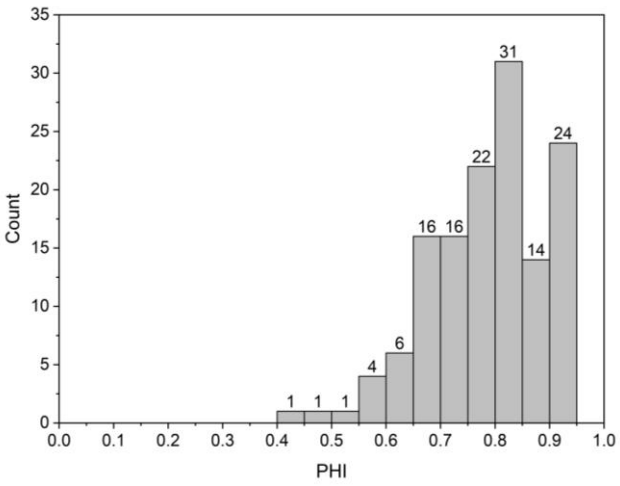

Figure 8. The distribution of PHI value of extracted validation points

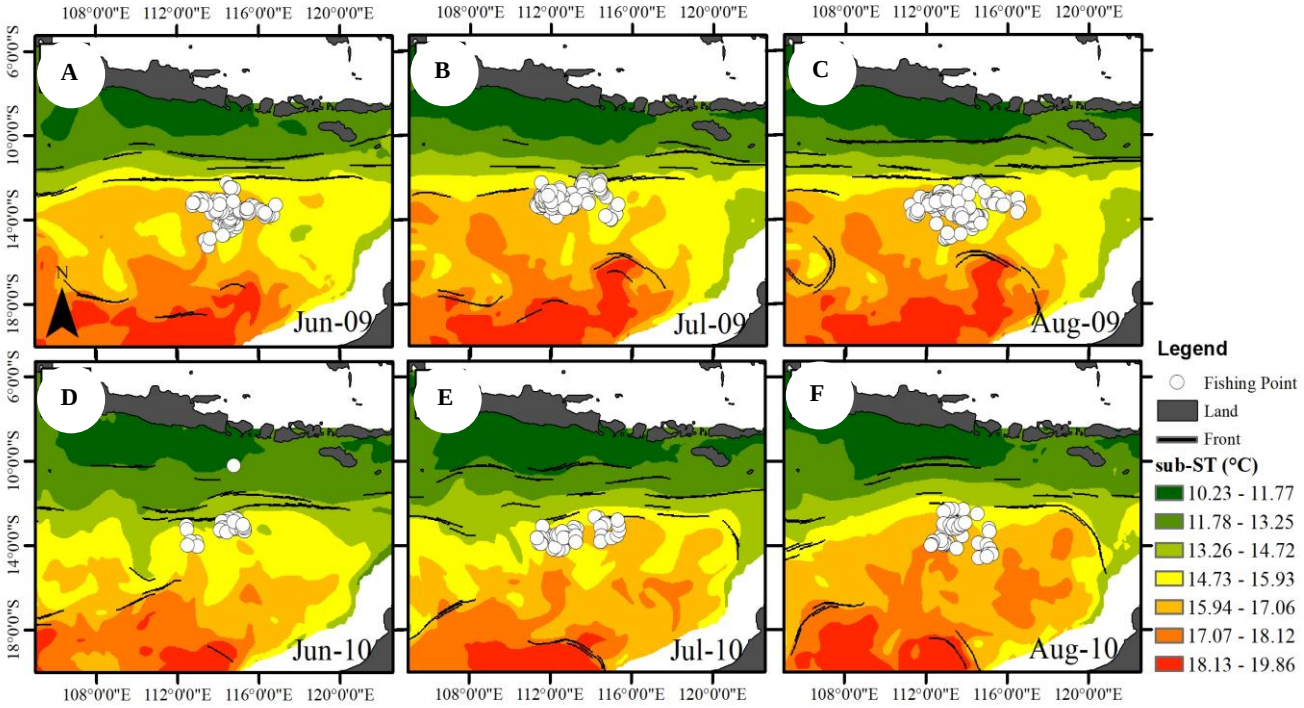

Figure 9. The thermal front maps for peak season in June, July, and August 2009 and 2010, overlain with the *T. obesus* fishing points (white circles). Blank white area represents no data

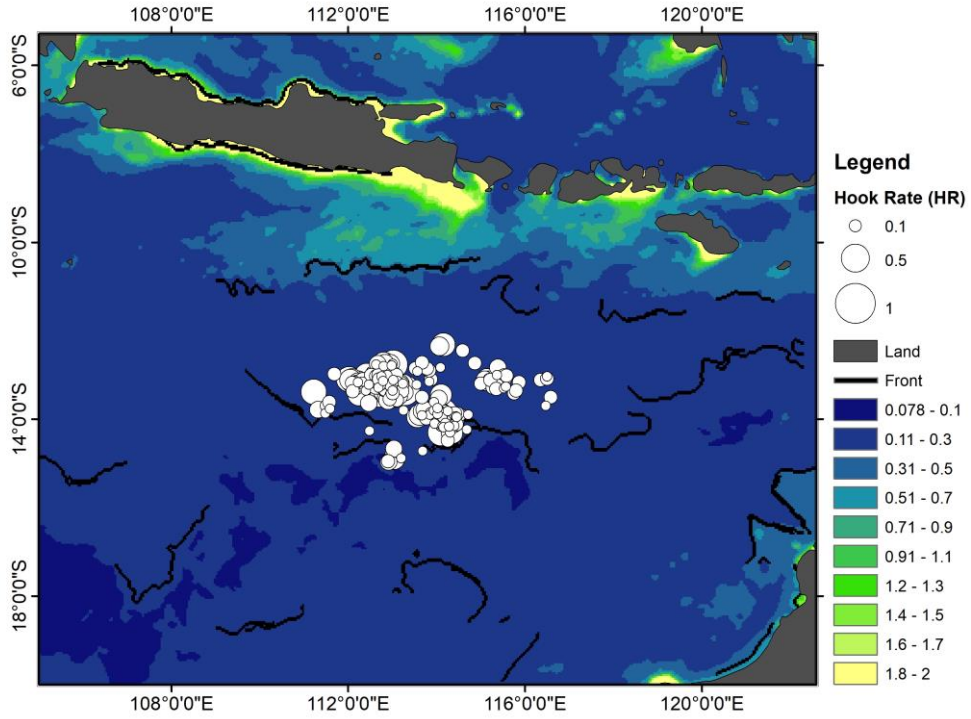

Figure 10. The SSC front on the southeast monsoon period occurred in the peak season of August 2009 and overlain with the *T. obesus* fishing points (white circles)

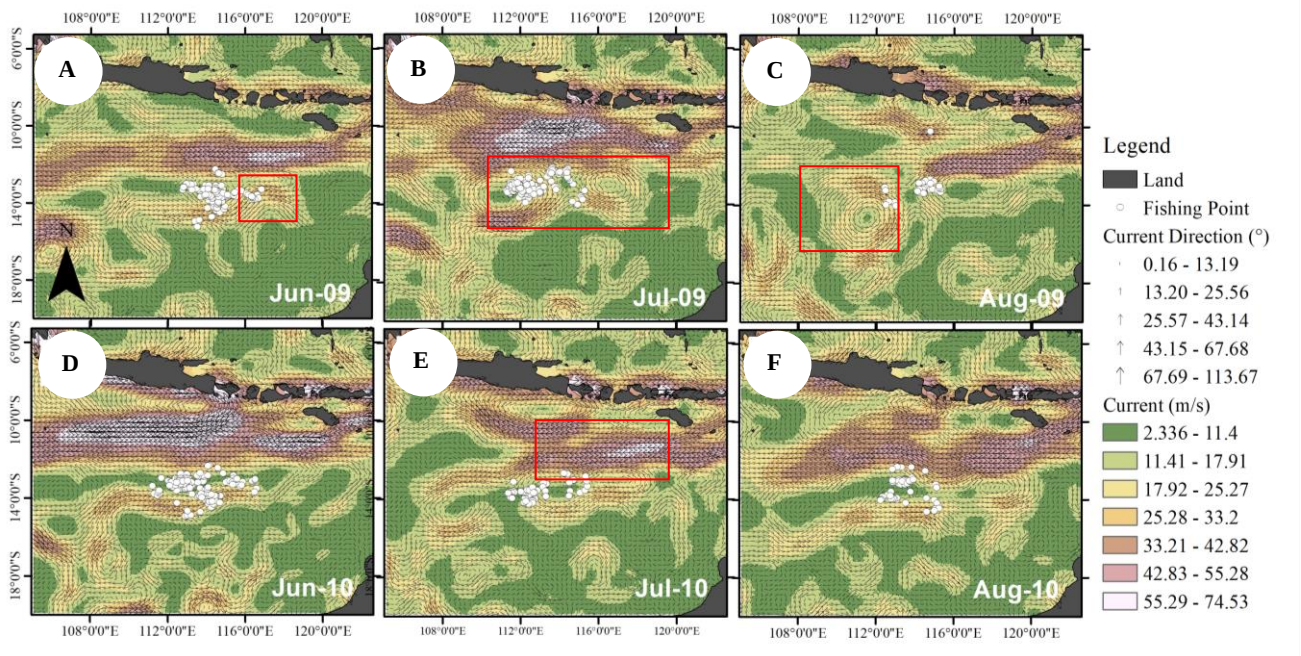

Figure 11. Current speed and direction in the study area for peak season (June, July, and August) in (A, B, C) 2009 and (D, E, F) in 2010, respectively, overlain with the *T. obesus* fishing points (white circles) and eddies (red square)

The FMA 573-EIO also presents significant challenges and opportunities for developing numerous applications that integrate numerical techniques, satellite data, in-situ data, and catch data to forecast the dynamics of water conditions and identify viable fishing grounds (Jayawiguna et al. 2019). Following research by Zainuddin et al. (2019), skipjack tuna distribution patterns follow its preferred area. This habitat suitability modeling opens up opportunities for future research into the distribution direction of bigeye tuna in the EIO. New ways to find possible fishing sites and

distributions are now achievable through analytical advancements. PHI may be a new option with reliable results for identifying the preferred habitat of the fish species. Using rich data sources combined with advanced technologies, implementing this approach can be highly helpful for discovering possible fishing zones and managing them to promote sustainable fishing development. Despite being considered a renewable resource, its abundance and capacity to survive may be impacted by the rising level of global tuna catches. As a result, tuna management and conservation are crucial (Pillai and Satheeshkumar 2012), along with efforts to continuously track fish stocks, such as evaluating the growth aspect to calculate fishing mortality (Fu et al. 2023). In addition to enhancing the effectiveness of fishing operations, prediction maps of potential habitat areas can be used as a guide for selecting the best fishing area and fishing closure.

Our findings conclude that SSC was the most influential habitat predictor for bigeye tuna distribution, followed by sub-ST, SSH, and sub-SS. Using these variables, our model can accurately predict the high suitable area of the highest bigeye catches, indicated by increased PHI. The bigeye tuna habitat prediction may strongly associate with features such as eddies and fronts that played an essential role in forming bigeye tuna habitat in the EIO.

ACKNOWLEDGEMENTS

We thank the Indonesia fishing fleet company, PT. Perikanan Nusantara Benoa, Bali for providing the fishery datasets. We acknowledge using chlorophyll-a data from the ocean color data distributed by NASA Ocean Color, sea temperature, salinity, sea surface height from Marine Copernicus, and current data from AVISO.

REFERENCES

Arrate IA, Fraile I, Marsac, Farley JH, Ezpeleta NR, Davies CR, Clear NP, Grewe P, Murua H. 2021. A review of the fisheries, life history and stock structure of tropical tuna (Skipjack *Katsuwonus Pelamis*, Yellowfin *Thunnus albacares* and Bigeye *Thunnus obesus*) in the Indian Ocean. Adv Mar Biol 88: 39-89. DOI: 10.1016/bs.amb.2020.09.002.

Baharuddin NAI, Zainuddin M, Najamuddin. 2022. The impact of ENSO-IOD on *Decapterus* spp. in Pangkajene Kepulauan and Barru Waters, Makassar Strait, Indonesia. Biodiversitas 23 (11):5613-5622. DOI: 10.13057/biodiv/d231110.

Bahtiar A, Barata A, Novianto D. 2013. Distribution of the hook rate of tuna longline in the Indian Ocean. Jurnal Penelitian Perikanan Indonesia 19 (4): 195-202. [Indonesian]

Bakun A. 2006. Fronts and eddies as key structures in the habitat of marine fish larvae: Opportunity, adaptive response and competitive advantage. Sci Mar 70S2: 105-22. DOI: 10.3989/scimar.2006.70s2105.

Behera S, Brandt P, Reverdin G. 2013. The Tropical ocean circulation and dynamics. In: Siedler G, Griffies SM, Gould J, Church JA (eds). Ocean Circulation and Climate. Academic Press, Massachusetts. DOI: 10.1016/B978-0-12-391851-2.00015-5.

Belkin IM. 2021. Review remote sensing of ocean fronts in marine ecology and fisheries. Remote Sens 13 (5): 1-22. DOI: 10.3390/rs13050883.

Block BA, Stevens ED. 2001. Tuna Physiology, Ecology, and Evolution. Academic Press, California.

Brill RW, Bigelow KA, Musyl MK, Fritsches KA, Warrant EJ. 2005. Bigeye tuna (*Thunnus obesus*) behavior and physiology and their relevance to stock assessments and fishery biology. Coll Vol Sci Pap Int Comm Cons Atl Tunas 57 (2):142-61.

Cai LN, Xu LL, Tang DL, Shao WZ, Liu Y, Zuo JC, Ji QY. 2020. The effects of ocean temperature gradients on bigeye tuna (*Thunnus obesus*) distribution in the equatorial Eastern Pacific Ocean. Adv Space Res 65 (12): 2749-60. DOI: 10.1016/j.asr.2020.03.030.

Chapman CC, Lea MA, Meyer A, Sallée JB, Hindell M. 2020. Defining Southern Ocean fronts and their influence on biological and physical processes in a changing climate. Nat Clim Change 10 (3): 209-19. DOI: 10.1038/s41558-020-0705-4.

Fu D, DeBruyn P, Fiorellato F, Nelson L, Pierre L, FernandezDiaz C, Chassot E. 2023. Assessing the impact of growth on estimates of fishing mortality-An Illustration with Indian Ocean Bigeye Tuna. Reg Stud Mar Sci 62: 102981. DOI: 10.1016/j.rsma.2023.102981.

Gaertner D, Guéry L, Goñi N, Amande J, Alayon PP, N'Gom F, Pereira J, Addi E, Ailloud L, Beare D. 2022. Tag-shedding rates for tropical tuna species in the Atlantic Ocean Estimated from Double-Tagging Data. Fish Res 248: 106211. DOI: 10.1016/j.fishres.2021.106211.

Gaol JL, Leben RR, Vignudelli S, Mahapatra K, Okada Y, Nababan B, Ling MM, Amri K, Arhatin RE, Syahdan M. 2015. Variability of Satellite-derived sea surface height anomaly, and its relationship with bigeye tuna (*Thunnus obesus*) catch in the Eastern Indian Ocean. Eur J Remote Sens 48: 465-77. DOI: 10.5721/EuJRS20154826.

Gaol JL, Mahapatra K, Okada Y, Pasaribu BP, Manurung D, Nurjaya IW. 2002. Fish catch relative to environmental parameters observed from satellite during ENSO and dipole mode events 1997/98 in the South Java Sea. PORSEC BALI 407-13.

Gingele FX, Deckker PD, Girault A, Guichard F. 2002. History of the South Java current over the Past 80 Ka. Palaeogeogr Palaeoclimatol Palaeoecol 183 (3-4): 247-260. DOI: 10.1016/S0031-0182(01)00489-8.

Gordon AL. 2005. Oceanography of the Indonesian Seas and their throughflow. Oceanography (Wash.D.C.) 18 (4): 14-27. DOI: 10.5670/oceanog.2005.18.

Guisan A, Edwards Jr TC, Hastie T. 2002. Generalized linear and generalized additive models in studies of species distributions: setting the scene. Ecol Modell 157: 89-100. DOI: 10.1016/S0304-3800(02)00204-1.

Haghi VA, Zarkami R, Sadeghi R, Fazli H. 2016. Modeling Habitat Preferences of *Caspian kutum, Rutilus frisii kutum* (Kamensky, 1901) (Actinopterygii, Cypriniformes) in the Caspian Sea. Hydrobiologia 766 (1):103-19. DOI: 10.1007/s10750-015-2446-3.

Hapsari AT. 2006. Optimization of tuna Catching Business Production Post Fuel Price Increase at PT. Perikanan Samodra Besar, Benoa, Bali. [Thesis]. Institut Pertanian Bogor, Bogor. [Indonesian]

Hastie T, Tibshirani R. 1987. Generalized Additive Models: Some applications. J Am Stat Assoc 83: 371-386. DOI: 10.1080/01621459.1987.10478440.

Hidayat R, Zainuddin M, Safruddin S, Mallawa A, Farhum SA. 2019. Skipjack tuna (*Katsuwonus pelamis*) Catch in relation to the thermal and chlorophyll-a fronts during May - July in the Makassar Strait. IOP Conf Ser: Earth Environ Sci 253 (1). DOI: 10.1088/1755-1315/253/1/012045.

IOTC. 2021. Executive summary: bigeye tuna. https://iotc.org/science/status-summary-species-tuna-and-tuna-species-under-iotc-mandate-well-other-species-impacted-iotc, accessed on January 2023.

Hastie TJ, Tibshirani RJ. 1990. Generalized Additive Models. Chapman & Hall/CRC, New York/Boca Raton.

Holland KN, Sibert JR. 1994. Physiological thermoregulation in bigeye tuna, *Thunnus obesus*. Environ Biol Fish 40:319-327. DOI: 10.1007/BF00002520.

Jatmiko I, Setyadji B, Novianto D. 2014. Spatial and temporal distribution of bigeye tuna (*Thunnus obesus*) in the Eastern Indian Ocean. Jurnal Lit. Perikanan Indonesia 20 (3):137-42. [Indonesian]

Jayawiguna MH, Triyono, Wibowo S. 2019. Overview of Potential, Development, and Challenges in the Utilization of Marine and Fisheries Resources in FMA 573. In: Wibowo W, Jayawiguna MH, Triyono (eds). Potensi sumberdaya kelautan dan perikanan WPPNRI 573. AMAFRAD Press, Jakarta. [Indonesian]

Johnson JB, Omland KS. 2004. Model selection in ecology and evolution. Trends Ecol Evol 19 (2):101-108. DOI: 10.1016/j.tree.2003.10.013.

Kim J, Na H. 2022. Interannual variability of yellowfin tuna (*Thunnus albacares*) and bigeye tuna (*Thunnus obesus*) catches in the Southwestern Tropical Indian Ocean and its relationship to climate variability. Front Mar Sci 9. DOI: 10.3389/fmars.2022.857405.

Kumar PS, Pillai GN, Manjusha U. 2014. El Nino Southern Oscillation (ENSO) impact on tuna fisheries in Indian Ocean. Springer Plus 3 (1): 591. DOI: 10.1186/2193-1801-3-591.

Lan KW, Wu YL, Chen LC, Naimullah M, Lin TH. 2021. Effects of climate change in marine ecosystems based on the spatiotemporal age structure of top predators: A case study of bigeye tuna in the Pacific Ocean. Front Mar Sci 8. DOI:10.3389/fmars.2021.614594.

Lee D, Son SH, Kim W, Park JM, Joo H, Lee SH. 2018. Spatio-temporal variability of the habitat suitability index for chub mackerel (*Scomber japonicus*) in the East/Japan Sea and the South Sea of South Korea. Remote Sens 10 (6). DOI: 10.3390/rs10060938.

Lee MA, Weng JS, Lan KW, Vayghan AH, Wang YC, Chan JW. 2020. Empirical habitat suitability model for immature albacore tuna in the North Pacific Ocean obtained using multisatellite remote sensing data. Intl J Remote Sens 41 (15): 5819-37. DOI: 10.1080/01431161.2019.1666317.

Ministry of Marine Affairs and Fisheries (MMAF). 2022. Roadmap Preparation of Indonesia Ocean Accounts. Kementrian Kelautan Perikanan, Jakarta.

Meyers G. 1996. Variation of Indonesian throughflow and the El Niño-Southern Oscillation. J Geophys Res Oceans 101 (C5): 12255-12263. DOI: 10.1029/95JC03729.

Mugo R, Saitoh SI. 2020. Ensemble modelling of skipjack tuna (*Katsuwonus pelamis*) habitats in the western north pacific using satellite remotely sensed data; a comparative analysis using machine-learning models. Remote Sens 12 (16). DOI: 10.3390/SU12166419.

Nugraha B, Hufiadi. 2012. Tuna longline fisheries productivity in Benoa (Case Study: PT. Perikanan Nusantara). Mar Fisheries 3 (2):135-140. DOI: 10.29244/jmf.3.2.135-140.

Nugraha B, Triharyuni S. 2009. The influence of temperature and depth of tuna longline fishing hooks on tuna catch results in the Indian Ocean. Jurnal Penelitian.Perikanan Indonesia 15 (3):239-47. [Indonesian]

Nurani TW, Wahyuningrum PI, SH Wisudo, Gigentika S, Arhatin RE. 2018. Model designs of Indonesian tuna fishery management in the Indian Ocean (FMA 573) using soft system methodology approach. Egypt J Aquat Res 44 (2):139-44. DOI: 10.1016/j.ejar.2018.06.005.

Oliver MA, Webster R. 1990. Kriging: A method of interpolation for geographical information systems. Intl J Geogr Inf Syst 4 (3): 313-332. DOI: 10.1080/02693799008941549.

Pillai NG, Satheeshkumar P. 2012. Biology, fishery, conservation and management of Indian Ocean Tuna Fisheries. Ocean Sci J 47 (4): 411-433http://dx.doi.org/10.1007/s12601-012-0038-y.

Rochman F, Jatmiko I, Fahmi Z. 2018. Dynamics of the tuna longline industry at Benoa Port. Mar Fishery 9 (2):209-220. DOI: 10.29244/jmf.9.2.209-220. [Indonesian]

Safruddin, Hidayat R, Farhum SA, Zainuddin M. 2022. The Use of Statistical Models in identifying skipjack tuna habitat characteristics during the southeast monsoon in the Bone Gulf, Indonesia. Biodiversitas 23 (4): 2231-37. DOI: 10.13057/biodiv/d230459.

Sambah, AB, Izzah AN, Intyas CA, Widhiyanuriyawan D, Affandy DP, Wijaya A. 2023. Analysis of the Effect of ENSO and IOD on the productivity of yellowfin tuna (*Thunnus albacares*) in the South Indian Ocean, East Java, Indonesia. Biodiversitas 24 (5): 2689-2700. DOI: 10.13057/biodiv/d240522.

Scales KL, Miller PI, Embling CB, Ingram SN, Pirotta E, Votier SC. 2014. Mesoscale fronts as foraging habitats: composite front mapping reveals oceanographic drivers of habitat use for a pelagic seabird. J R Soc Interface 11 (100). DOI: 10.1098/rsif.2014.0679.

Schaefer KM, Fuller DW. 2022. Horizontal movements, utilization distributions, and mixing rates of yellowfin tuna (*Thunnus albacares*) tagged and released with archival tags in six discrete areas of the Eastern and Central Pacific Ocean. Fish Oceanogr 31 (1): 84-107. DOI: 10.1111/fog.12564.

Senina I, Lehodey P, Sibert J, Hampton J. 2019. Integrating tagging and fisheries data into a spatial population dynamics model to improve its predictive skills. Can J Fish Aquat Sci 77 (3): 576-593. DOI: 10.1139/cjfas-2018-0470.

Setiawati MD, Miura F. 2014. Sea surface temperature and sea surface chlorophyll in relation to bigeye tuna fishery in the southern waters off Java and Bali. The 12th Biennial Conference of Pan Ocean Remote Sensing Conference (PORSEC). Bali, 4-7 November 2014.

Setiawati MD, Sambah AB, Miura F, Tanaka T, As-Syakur AR. 2015. Characterization of bigeye tuna habitat in the Southern Waters off Java-Bali using remote sensing data. Adv Space Res 55 (2): 732-46. DOI: 10.1016/j.asr.2014.10.007.

Sudre F, Dewitte B, Mazoyer C, Garçon V, Sudre J, Penven P, Rossi V. 2023. Spatial and seasonal variability of horizontal temperature fronts in the mozambique channel for both epipelagic and mesopelagic realms. Front Mar Sci 9. DOI: 10.3389/fmars.2022.1045136.

Syah AF, Gaol JL, Zainuddin M, Apriliya NR, Berlianty D, Mahabror D. 2019. Habitat model development of bigeye tuna (*Thunnus obesus*) during Southeast Monsoon in the Eastern Indian Ocean Using Satellite Remotely Sensed Data. IOP Conf Ser: Earth Environ Sci 276: 012011. DOI: 10.1088/1755-1315/276/1/012011.

Syah AF, Saitoh SI, Alabia ID, Hirawake T. 2016. Predicting potential fishing zones for pacific saury (*Cololabis saira*) with Maximum Entropy Models and Remotely Sensed Data. Fish Bull 114 (3): 330-342. DOI: 10.7755/FB.114.3.6.

Syamsuddin ML, Saitoh SI, Hirawake T, Samsul B, Harto AB. 2013. Effects of El Niño-Southern Oscillation events on catches of bigeye tuna (*Thunnus obesus*) in the Eastern Indian Ocean off Java. Fish Bull 111 (2): 175-88. DOI: 10.7755/FB.111.2.5.

Vinogradova N, Lee T, Boutin J,Drushka K, Fournier S, Sabia R,Stammer D, Bayler E, Reul N,Gordon A, Melnichenko O, Li L,Hackert E, Martin M, Kolodziejczyk N,Hasson A, Brown S, Misra S andLindstrom E. 2019. Satellite Salinity Observing System: Recent Discoveries and the Way Forward. Front Mar Sci 6: 243. DOI: 10.3389/fmars.2019.00243.

Wang X, Wang C. 2014. Different impacts of various el niño events on the Indian Ocean Dipole. Climate Dynamics 42 (3):991-1005. DOI: 10.1007/s00382-013-1711-2.

Wood SN. 2017. Generalized Addtive Models: An Introduction with R Second Edition. CRC Press, United Kingdom.

Wright SR, Righton D, Naulaerts J, Schallert RJ, Bendall V, Griffiths C, Castleton M, Gutierrez DD, Madigan D, Beard A, Clingham E, Henry L, Laptikhovsky V, Beare B, Thomas W, Block BA, Collins MA. 2021. Fidelity of Yellowfin Tuna to Seamount and Island Foraging Grounds in the Central South Atlantic Ocean. Deep Sea Res Part I: Oceanogr Res Pap 172. DOI: 10.1016/j.dsr.2021.103513.

Zainuddin M, Farhum A, Safruddin S, Selamat MB, Sudirman S, Nurdin N, Syamsuddin M, Ridwan M, Saitoh SI. 2017. Detection of pelagic habitat hotspots for skipjack tuna in the Gulf of Bone-Flores Sea, Southwestern Coral Triangle Tuna, Indonesia. PLoS ONE 12 (10): 1-19. DOI: 10.1371/journal.pone.0185601.

Zainuddin M, Farhum SA, Safruddin S, Hidayat R, Putri ARS, Ridwan M. 2021. Dynamics of thermal fronts distribution in the Flores Sea, Indonesia: An implication for locating potential skipjack tuna fishing ground. IOP Conf Ser: Earth Environ Sci 763 (1): 012045. DOI: 10.1088/1755-1315/763/1/012045.

Zainuddin M, Safruddin S, Farhum A, Budimawan B, Hidayat R, Ihsan YN. 2023. Satellite-Based ocean color and thermal signatures defining habitat hotspots and the movement pattern for commercial skipjack tuna in Indonesia Fisheries Management Area 713, Western Tropical Pacific. Remote Sens 15 (5): 1268. DOI: 10.3390/rs15051268.

Zainuddin M, Saitoh K, Saitoh SI. 2008. Albacore (*Thunnus alalunga*) fishing ground in relation to oceanographic conditions in the Western North Pacific Ocean using Remotely Sensed Satellite Data. Fish Oceanogr 17 (2): 61-73. DOI: 10.1111/j.1365-2419.2008.00461.x.

Zhang T, Song L, Yuan H, Song B, Ngando NE. 2021. A comparative study on habitat models for adult bigeye tuna in the indian ocean based on gridded tuna longline fishery data. Fish Oceanogr 30 (5): 584-607. DOI: 10.1111/fog.12539.